Supplemental Figure 1

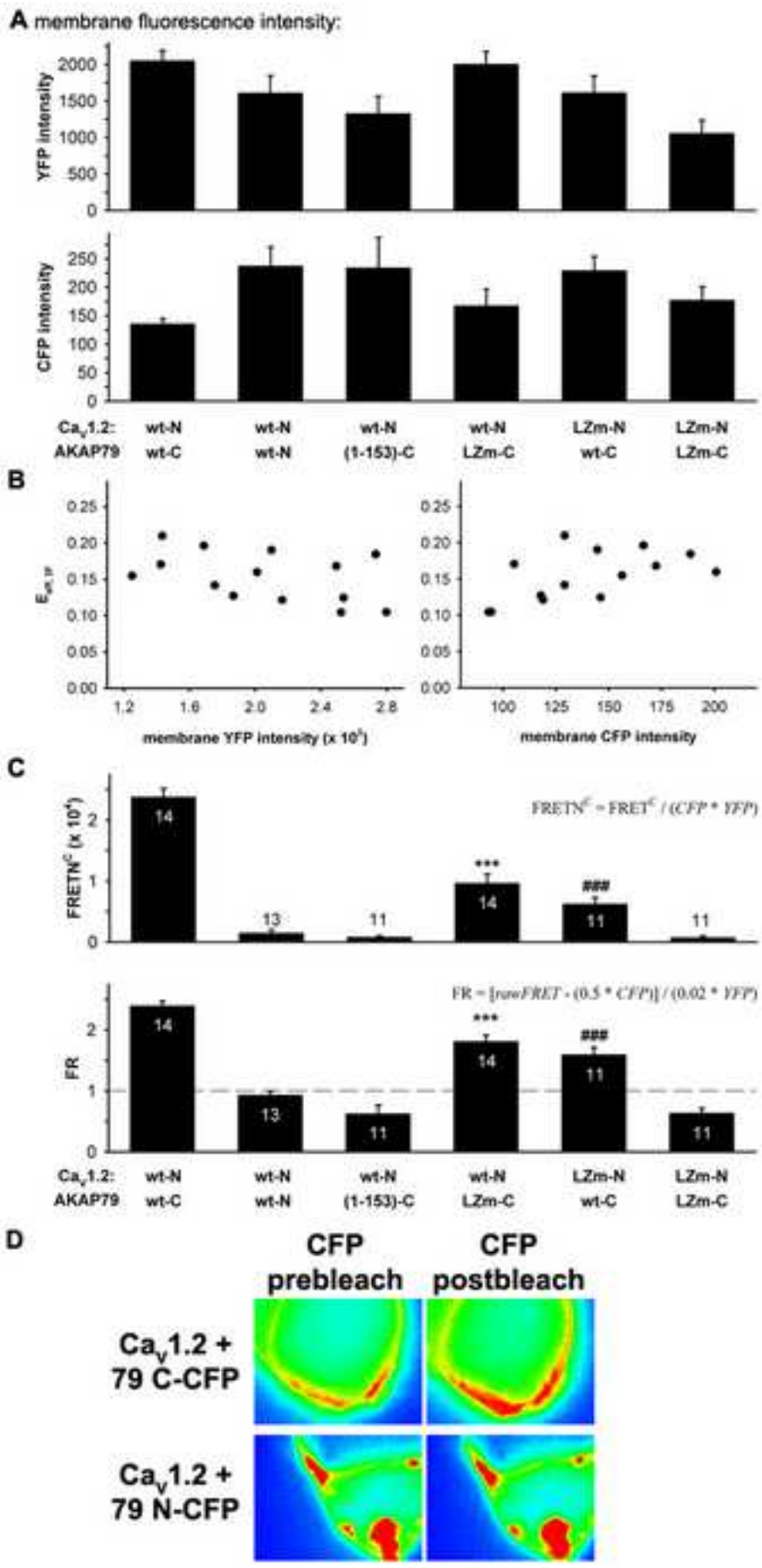

Supplemental Figure S1, *Oliveria et al.*

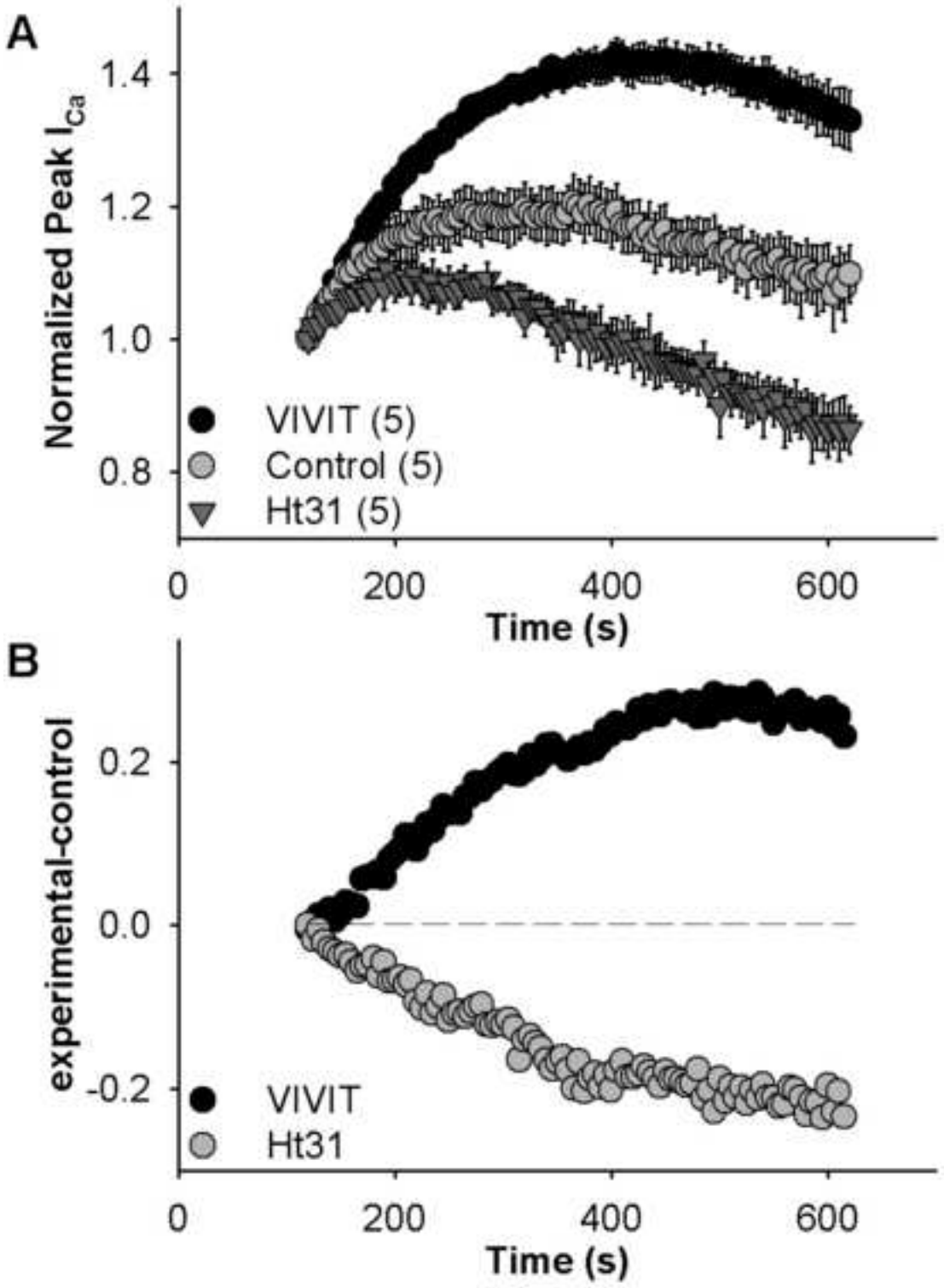

Supplemental Figure S2, *Oliveria et al.*

Supplemental Figure

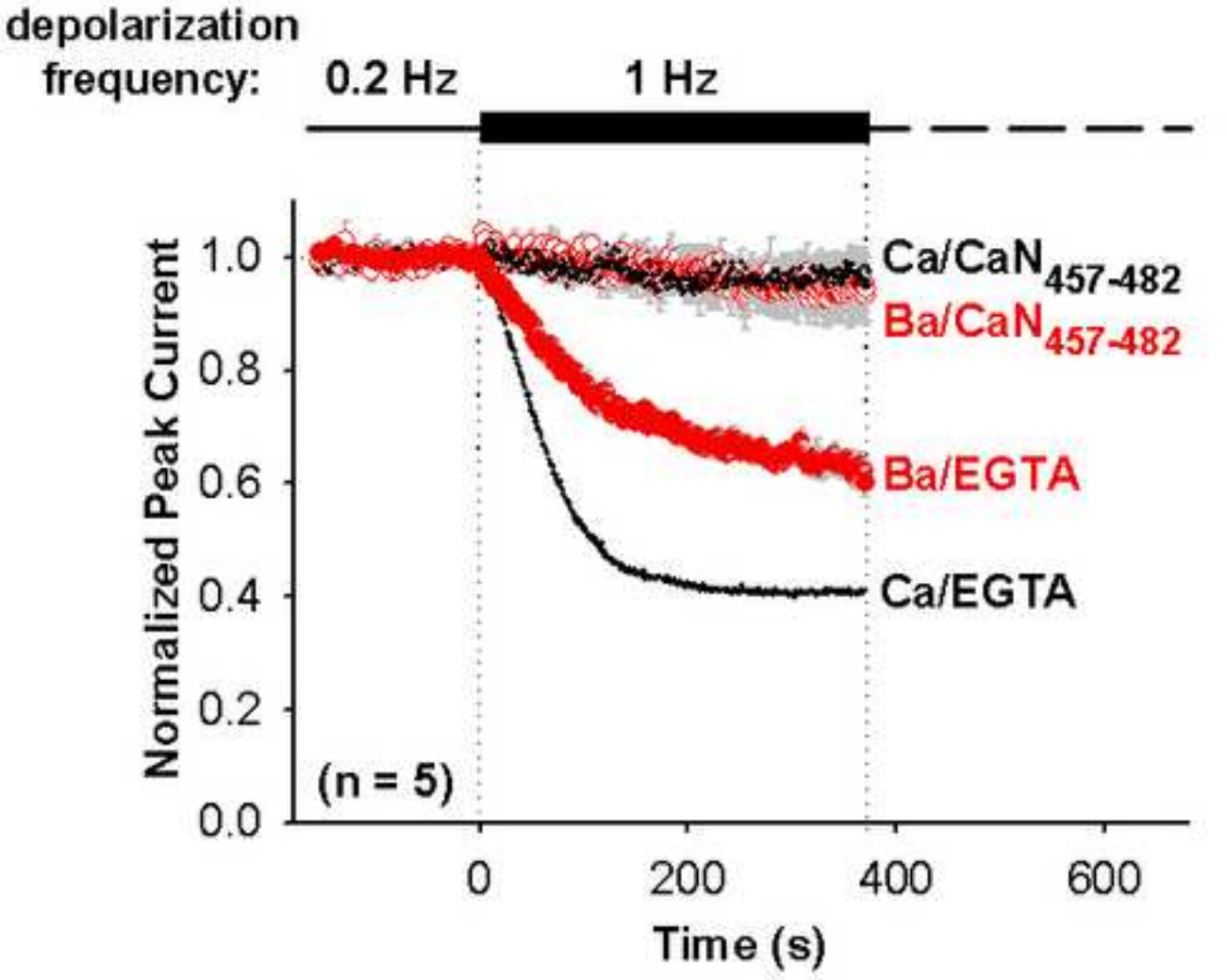

Figure S3, *Oliveria et al.*

Supplemental Table S1. Current density values

Transfected HEK293 cells[a]		
$Ca_V1.2$	AKAP79	pA/pF (± s.e.m.)
wt	wt	40.6 (6.3)
"	79^{pro2}	35.4 (6.4)
"	79ΔCaN	32.7 (10.8)
"	79ΔPIX	37.7 (5.3)
S1928A	wt	36.6 (5.4)
LZm	LZm	21.7 (5.0)*
Cultured Hippocampal Neurons[b]		
Condition		pA/pF (± s.e.m.)
+FSK		18.6 (2.3)
–FSK		22.8 (3.0)
150RNAi +FSK		20.7 (3.1)
150RNAi –FSK		19.6 (1.5)
79wt Rescue (+FSK)		8.7 (1.2)*
79ΔPIX Rescue (+FSK)		10.5 (3.0)*

*$P < 0.05$ relative to upper row of data

a, peak current values obtained from stabilized baseline value at 0.2 Hz prior to stearated peptide application

b, peak current values obtained 1 min after establishing the whole cell recording configuration

SUPPLEMENTAL MATERIAL

Supplemental Experimental Procedures

FRET measurements

Fluorescence images were acquired 2-3 days post-transfection using a Nikon TE-300 inverted microscope equipped with a 175 W xenon illumination source, 100x oil-immersion objective lens, 16 MHz CCD camera (SensiCam QE, Cooke) and dual filter wheels (Sutter Instruments) controlled by SlideBook 4.0 software (Intelligent Imaging Innovation). For sensitized FRET measurements ($FRET^C$, 3F), an 86002 (JP4) dichroic mirror (Chroma) and three different filter sets (donor/CFP, acceptor/YFP, and raw FRET) were used to capture serially a set of three images from a fixed image plane. The three images were captured using the same exposure time (100 ms in some experiments, 250 ms in others). The three filter sets used were: donor (*CFP*; 436 center excitation wavelength and 10 nm bandwidth (436/10 nm), emission 470/30 nm), acceptor (*YFP*; excitation 500/20 nm, emission 535/30 nm), and FRET (*rawFRET*; excitation 436/10 nm, emission 535/30 nm). Light that has passed through the FRET filter set is contaminated by donor bleed through (average fraction = 0.50) and acceptor cross-excitation (average fraction = 0.02); fractional contamination by bleed through and cross-excitation were determined in separate experiments using cells that expressed CFP- or YFP-tagged constructs alone. Corrected, sensitized FRET ($FRET^C$) images were obtained by subtracting the contamination components, pixel-by pixel, from raw FRET images using the following equation (adapted from Gordon et al., 1998):

$$FRET^C = rawFRET - (0.50 * CFP) - (0.02 * YFP).$$

To obtain estimates of effective FRET efficiency (E_{eff}) from images, Slidebook 4.0 was used to draw masks that isolated in-focus, membrane-localized fluorescence. From masked raw FRET, CFP and YFP images, the FRET ratio (*FR*) was extracted as:

$$FR = [rawFRET - (0.5 * CFP)] / (0.02 * YFP).$$

E_{eff} was then calculated as:

$$E_{eff,\,3F} = (FR - 1) * (\varepsilon_{YFP440} / \varepsilon_{CFP440}),$$

where ε_{YFP440} and ε_{CFP440} represent the average molar extinction coefficients for YFP and CFP over the band pass of the CFP excitation filter. E_{eff} takes into account cell-to-cell variation in expression of YFP and CFP, so that this FRET index is effectively independent of donor and acceptor concentration (Erickson et al., 2003).

FRET was additionally estimated using an acceptor photobleach (PB) method. PB measurements were obtained from the same cells used to make the 3F measurements. PB FRET was measured as the difference between membrane-localized CFP (donor) fluorescence intensity before and after photobleach of YFP (acceptor). Photobleach was achieved by 3 min continuous illumination at 535 nm, and was virtually complete. E_{eff} was calculated from acceptor photobleach images as:

$$E_{eff,\,PB} = 1 - (F_{DA}/F_{D}),$$

where F_{DA} and F_{D} indicate donor intensity before and after photobleaching, respectively (E_{eff} calculations adapted from Erickson et al., 2003).

Legends for Supplemental Figures

Figure S1. Analysis of FRET between AKAP79-CFP and $Ca_V1.2$-YFP.

(**A**) Average fluorescence intensity for plasma membrane-localized CFP and YFP. For these analyses, the plasma membrane region of each cell was defined by a mask that closely bounded the irregular ring of the plasma membrane. Masks for each cell analyzed were constructed using Slidebook software. The fluorescence intensities obtained from the masked regions were used to calculate $E_{\text{eff, 3F}}$ values in Figure 1.

(**B**) $E_{\text{eff, 3F}}$ for the $Ca_V1.2$ N-YFP AKAP79 C-CFP pairing (upper row of data in Figure 1C and D) is not dependent upon donor or acceptor expression levels over the range of intensities studied.

(**C**) Top, data from Figure 1D, normalized using the $FRETN^C$ formalism. $FRETN^C$ is proportional to the equilibrium constant for the binding interaction (Gordon et al., 1998): $FRETN^C = FRET^C / (CFP * YFP)$. Negative $FRETN^C$ values are obtained when there is no FRET due to overcorrection for CFP and YFP cross-bleed. Bottom, FR values used to calculate $E_{\text{eff, 3F}}$. An FR value >1 is indicative of energy transfer.

(**D**) Representative pseudocolor images showing CFP donor fluorescence intensity before (CFP prebleach) and after (CFP postbleach) YFP acceptor photobleaching for $Ca_V1.2$-YFP and AKAP79-CFP labeled at either the C-terminus (top row) or N-terminus (bottom row). Donor intensity increases after acceptor photobleaching in the top row of images, but not in the bottom row.

Figure S2. The effect of non-stearated anchoring inhibitor peptides.

(**A**) Time course of change in peak current amplitude when non-stearated anchoring inhibitor peptides were dialyzed into HEK293 cells transfected with $Ca_V1.2$ subunits and AKAP79-YFP and stimulated with FSK. Current amplitude normalized to the value obtained 2 min after establishing the whole cell recording configuration.

(**B**) After correction for the run-up and run-down of current observed for the average control time course, the effects of non-stearated anchoring inhibitor peptides on $Ca_V1.2$ current amplitude are similar those of the stearated versions illustrated in **Figures 2** and **3**.

Figure S3. Reversal by CaN of FSK enhancement of $Ca_V1.2$ current is weakly activated by Ba^{2+}.

Peak inward current amplitude in response to changes in step depolarization frequency, as in **Figure 4**, when extracellular Ca^{2+} was replaced with equimolar Ba^{2+}. Pipet solution contained 10 mM EGTA, or CaN autoinhibitory peptide + 10 mM EGTA. Time courses corrected for the rate of channel rundown at 0.2 Hz prior to 1 Hz stimulation. Error bars, representing s.e.m., are plotted in gray. Small dots replicate data presented in **Figure 4**.